Mathematical Biosciences and Engineering

MBE, 16(6): 7230–7249.
DOI: 10.3934/mbe.2019363
Received: 29 April 2019
Accepted: 01 July 2019
Published: 08 August 2019

http://www.aimspress.com/journal/MBE

Research article

Free vibration of summation resonance of suspended-cable-stayed beam

Chunguang Dong[1], Zhuojie Zhang[2,3,*], Xiaoxia Zhen[4] and Mu Chen[4]

[1] Poly ChangDa Engineering Co., Ltd., Guangzhou511431, PR China
[2] School of Civil Engineering, Shi Jiazhuang Tiedao University, Shijiazhuang050043, PR China
[3] Innovation Center for Wind Engineering and Wind Energy Technology of Hebei Province, Shijiazhuang, Hebei 050043, PR China
[4] School of Civil Engineering and Transportation, South China University of Technology, Guangzhou510640, PR China

*** Correspondence:** Email: civilzhangzhuojie@163.com.

Abstract: Free vibration of summation resonance of suspended-cable-stayed beam is investigated in the article. A 3-DOF model of the coupled structure is built, with the main cable and sling (vertical cable) considered to be geometrically nonlinear, and the beam is taken as linear Euler beam. Hamilton's principle is used to derive the dynamic equilibrium equations of the coupled structure. Then, the dynamic equilibrium equations are solved by means of multiple scales method, the second order approximation solutions of single-modal motion of the coupled structure are obtained. Numerical examples are presented to discuss time history of free vibration of the summation resonance, with and without damping. Additionally, fourth-order Runge-Kutta method is directly used for the dynamic equilibrium equations to complement and verify the analytical solutions. The results show that the coupled structure performs strongly nonlinear and coupled characteristics, which is useful for engineering design.

Keywords: free vibration; summation resonance; multiple scales method; fourth-order Runge-Kutta method

1. Introduction

The sling or the vertical cable is widely used in suspension bridge. By connecting the main cable with the beam, the sling plays a decisive role in transmitting force. However, in recent years as the span of the suspension bridge increases, length of the sling also increases, which directly leads to protruding nonlinear characteristics of overall structures. Furthermore, the coupling among the sling, the main cable and the beam results in new mechanisms of the internal resonance. Therefore, the study of nonlinear characteristics of the sling, especially the coupled characteristics with other structural members, is of considerable importance to mechanical and structural engineers. In recent years, cable structures have been intensive study by many researchers all over the world. Among the known solutions of them, there are harmonic balance method [1,2], multiple scales method [3] (including discretization approach and direct approach), finite element method [4,5], finite difference method [6], numerical integration method [7] and experimental method [8].

Since the beginning research of cable, some articles only forced on a single cable [9–12], which can not reveal the totally nonlinear characteristics of the whole structure.

From the perspective of the overall structure, Sun and Wang [13] established a 2-DOF cable-beam coupled model by simplifying the cable to a taut string and reducing the beam to a mass-spring system; he proved the displacement curves of the cable and beam have the characteristic of "beat". Fujino and Warnitchai [14] established another kind of 3-DOF cable-beam coupled model; in this model, the beam was considered to be linear Euler beam, with one end point fixed and another end point connected to the cable, the cable was taken as string with sag. Based on the same model, Xia and Fujino [15] further studied the behavior of the system under a random excitation. Then, Xia et al. [16] established a cable finite element to analyze the nonlinear vibration of cables in cable-stayed bridge; by comparing with the available analytical solutions, they demonstrate that the cable finite element can capture nonlinear vibration, in particular auto-parametric vibration of stay cables under harmonic and random loadings. Gattulli [17,18] established the similar kind of cable-beam coupled model and studied linear and nonlinear behave of the system. Gattulli and Lepidi [19] set up a finite element model and verified the results of theoretical analysis and finite element model through experiments. By considering the nonlinearity of the beam, Wang et al. [20] researched the nonlinear behavior of the coupled system. Wei et al. [21] investigated the nonlinear dynamics of a cable-stayed beam driven by the sub-harmonic resonance of the beam and the principal parametric resonance of the cable. For the first time, Wang and Li [22] researched the nonlinearity of cable-beam coupled structure under the thermal loads. Kang et al. [23] discussed the effects of some key parameters of the stay cable, such as initial tension force, damping and inclination angle, and the excitation frequency and amplitude on the nonlinear behavior of the combination structure. With the method of transfer matrix, Zhao and Kang [24,25] investigated the free vibration of the cable-stayed arch bridge.

Though many papers had studied the nonlinear vibration of cable-beam coupled structure and got some available conclusions of coupled characteristics of cable and beam, they mainly forced on the cable-stayed bridge, in which the stay cable is only under one kind of excitation on one end point and the coupled model is 2-DOF. However, in suspension bridge, the sling or the vertical cable is under two kinds of excitation on two end points. To well understand the coupling among

the sling, the main cable and the beam, the coupled model will be 3-DOF. There exists new kind of internal resonance, such as summation resonance. This will be new and interesting topic for us.

About summation resonance, Nayfeh and Mook [26] introduced the fundamental theory of it, which can be used in many areas, such as ship engineering, civil engineering and so on. Zhao et al. [27] studied the summation resonance of a classic Spar platform under long periodic regular wave. Chen et al. [28] investigated the steady-state transverse vibration of a parametrically excited axially moving string with geometric nonlinearity and obtained the steady-state response of the summation resonance. There are also many other papers of summation resonance, which well guide us to introduce the theory of summation resonance into the suspension bridges.

In the paper, free vibration of summation resonance of the coupled structure is investigated with and without damping respectively. Firstly, a 3-DOF model is built, which treated the main cable and the sling as nonlinear taut string and the beam as Euler beam; secondly, Hamilton's principle and multiple scales method are used to derive and solve the dynamic equilibrium equations; thirdly, numerical integration method is used to discuss the nonlinear characteristics of the coupled structure. The conclusions show the three degrees of freedom strongly couple with each other and have the typical characteristics of "beat".

2. Derivation of governing equation

In order to simplify the problem, some assumptions are made in this paper, as follows:

The material nonlinearity of the coupled structure is not considered;

The sag curve of the main cable under gravity is approximately parabolic;

The flexural rigidity, torsional stiffness and shear stiffness of the main cable and sling are not considered;

The cable force of the main cable and sling are constant along the longitudinal direction;

The main cable and sling keep linear elastic during vibration.

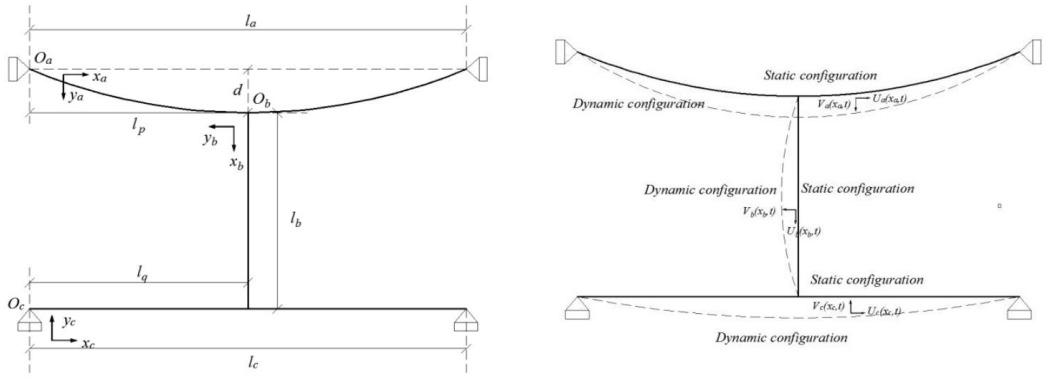

a b

Figure 1. Configuration of the coupled structure: a: reference; b: instantaneous.

In Figure 1, the Cartesian coordinate system is established, with the main cable descripted in the system of $o_a - x_a y_a$, the sling descripted in the system of $o_b - x_b y_b$, the beam descripted in the

system of $o_c - x_c y_c$; l_a, l_b and l_c donate the span of the main cable, sling and beam, respectively; l_p is the distance between the installation position of sling on the main cable and the left end of the main cable; l_q is the distance between the installation position of sling on the beam and the left end of the beam.

In particular, due to self-weight, the static configurations of the main cable, sling and beam exist. For simplicity, we neglect the contribution of static configurations of the sling and beam to the motion equations [29–31]. The static configuration of the main cable can be written as [32,33]:

$$y_a(x) = \frac{m_a g}{2H_a}\left(l_a x_a - {x_a}^2\right) \tag{1}$$

$$d = \frac{m_a g l_a^2}{8H_a} \tag{2}$$

where d is the sag of the main cable, H_a is the axial component of the initial cable force of the main cable.

The Lagrangian strain of the main cable and sling can be written as [30]:

$$\varepsilon_i = \frac{\partial x_i}{\partial s_i}\frac{\partial u_i}{\partial s_i} + \frac{\partial y_i}{\partial s_i}\frac{\partial v_i}{\partial s_i} + \frac{1}{2}\left(\frac{\partial v_i}{\partial s_i}\right)^2, i = a, b \tag{3}$$

According to Hamilton's principle and ignoring the movement of axial direction, the differential equation of lateral vibration of the coupled structure can be written as [18]:

$$m_a \ddot{v}_a + c_a \dot{v}_a - H_a v_a'' - \left(y'' + v_a''\right) h_a = F(t)\delta\left(x_a - l_p\right) \tag{4a}$$

$$m_b \ddot{v}_b + c_b \dot{v}_b - H_b v_b'' - v_b'' h_b = 0 \tag{4b}$$

$$m_c \ddot{v}_c + c_c \dot{v}_c + E_c I_c v_c^{(4)} = F(t)\delta\left(x_c - l_q\right) \tag{4c}$$

where m_a, m_b, m_c are the mass of the main cable, sling and beam per unit length; c_a, c_b, c_c are the damping coefficients of the main cable, sling and beam; v_a, v_b, v_c are the main cable, sling and beam displacement components in the lateral direction respectively; H_b is the axial component of the static cable force of the main cable and sling; E_c, I_c are the Young's modulus and moment of inertia of the cross section of the beam.

h_a and h_b are the increment in the axial component of cable force of the main cable and sling, which can be written as [30]:

$$h_a = \frac{E_a A_a}{l_a}\int_0^{l_a}\left[y_a' v_a' + \frac{1}{2}\left(v_a'\right)^2\right]dx_a \tag{5a}$$

$$h_b = \frac{E_b A_b}{l_b}\left\{-\left[v_c\left(l_q\right) + v_a\left(l_p\right)\right] + \frac{1}{2}\int_0^{l_b}\left(v_b'\right)^2 dx_b\right\} \tag{5b}$$

where A_a, A_b are the areas of the cross section of the main cable and sling.
$F(t)$ is dynamic cable force of the sling, which can be written as:

$$F(t) = H_b + h_b \tag{6}$$

For convenience, Eqs 4–6 is nondimensionalized by defining the following variables:

$$\begin{aligned} &\tilde{y} = \frac{y}{d}, \tilde{t} = \omega_0 t, \tilde{x}_i = \frac{x_i}{l_i}, \tilde{v}_i = \frac{v_i}{l_i}, \tilde{c}_i = \frac{c_i}{m_i \omega_0}, i = a,b,c \\ &\upsilon = \frac{d}{l_a}, \varsigma_1 = \frac{l_p}{l_a}, \varsigma_2 = \frac{l_q}{l_c}, \chi_1 = \frac{E_a A_a}{H_a}, \chi_2 = \frac{E_b A_b}{H_b} \\ &\kappa_1 = \frac{H_a}{\omega_0^2 m_a l_a^2}, \kappa_2 = \frac{H_b}{\omega_0^2 m_b l_b^2}, \kappa_3 = \frac{E_c I_c}{\omega_0^2 m_c l_c^4}, \omega_0 = 1.0\, rad/s \end{aligned} \tag{7}$$

Substituting Eq 7 into Eqs 4–6 yields

$$\ddot{v}_a + c_a \dot{v}_a - \kappa_1 \left[v_a'' - \chi_1 \left(\upsilon^2 y'' + v_a'' \right) \cdot e_a \right] = F(t) \delta(1 - \varsigma_1) \tag{8a}$$

$$\ddot{v}_b + c_b \dot{v}_b - \kappa_2 \left(v_b'' - \chi_2 v_b'' e_b \right) = 0 \tag{8b}$$

$$\ddot{v}_c + c_c \dot{v}_c + \kappa_3 v_c^{(4)} = F(t) \delta(1 - \varsigma_2) \tag{8c}$$

$$e_a = \int_0^1 \left[\upsilon y_a' v_a' + \frac{1}{2} (v_a')^2 \right] dx_a \tag{8d}$$

$$e_b = -\left[u_b(1) + u_b(0) \right] + \frac{1}{2} \int_0^1 (v_b')^2 dx_b \tag{8e}$$

$$F(t) = \kappa_2 (1 + \chi_2 e_b) \tag{8f}$$

The boundary conditions of the coupled structure can be written as:

$$v_a(0) = v_a(1) = 0 \tag{9a}$$

$$v_b(0) = v_b(1) = 0 \tag{9b}$$

$$v_c(0) = v_c(1) = v_c''(0) = v_c''(1) = 0 \tag{9c}$$

$$v_a(\varsigma_1) = u_b(0), v_c(\varsigma_2) = u_b(1) \tag{9d}$$

In the procedure of Galerkin, basis functions that satisfy boundary conditions are used. In order to investigate the coupling among the main cable, sling and beam, this paper only deals with single-modal lateral vibration of the coupled structure. Then the displacements are assumed as

$$v_i = q_i(t) \phi(x_i), \quad i = a,b,c \tag{10}$$

where $q_i(t)$ and $\phi(x_i)$ are the generalized coordinate and mode shape of the linearized problem of the coupled structure respectively.
Substituting Eq 10 into Eq 8 yields

$$\ddot{q}_a(t)+\mu_a\dot{q}_a(t)+\omega_a^2 q_a(t)=e_3H_b+e_4q_c(t)+e_5q_b^2(t)+e_6q_a^2(t)+e_7q_a^3(t) \tag{11a}$$

$$\ddot{q}_b(t)+\mu_b\dot{q}_b(t)+\omega_b^2 q_b(t)=f_3q_a(t)q_b(t)+f_4q_b(t)q_c(t)+f_5q_b^3(t) \tag{11b}$$

$$\ddot{q}_c(t)+\mu_c\dot{q}_c(t)+\omega_c^2 q_c(t)=m_3H_b+m_4q_a(t)+m_5q_b^2(t) \tag{11c}$$

The coefficients presented in Eq 11 are interpreted in the Appendix A.

In Eq 11, quadratic and cubic nonlinear terms simultaneously exist, showing strong nonlinearity. By square nonlinear term, the main cable and beam couple with the sling and provide parametric excitation for the sling, which produces many kinds of internal resonance. The summation resonance is one of them and will be discussed in the following sections.

3. Solution procedure

Both quadratic and cubic nonlinear terms are included in Eq 11, so the method of multiple scales can be used to solve the dynamic equilibrium equations. A small parameter ε should be introduced so that the damping and constant terms appear in the same perturbation equation. Eq 11 is then rewritten as

$$\ddot{q}_a(t)+\mu_a\varepsilon\dot{q}_a(t)+\omega_a^2 q_a(t)=e_3\varepsilon^3H_b+\varepsilon e_4q_c(t)+e_5q_b^2(t)+e_6q_a^2(t)+e_7q_a^3(t) \tag{12a}$$

$$\ddot{q}_b(t)+\mu_b\varepsilon\dot{q}_b(t)+\omega_b^2 q_b(t)=f_3q_a(t)q_b(t)+f_4q_b(t)q_c(t)+f_5q_b^3(t) \tag{12b}$$

$$\ddot{q}_c(t)+\mu_c\varepsilon\dot{q}_c(t)+\omega_c^2 q_c(t)=m_3\varepsilon^3H_b+m_4\varepsilon q_a(t)+m_5q_b^2(t) \tag{12c}$$

Introducing the time scales

$$T_n=\varepsilon^n t,\qquad n=0,1,2 \tag{13}$$

an approximate solution can be given by

$$q_a(t)=\varepsilon q_{a11}(T_0,T_1,T_2)+\varepsilon^2 q_{a12}(T_0,T_1,T_2)+\varepsilon^3 q_{a13}(T_0,T_1,T_2) \tag{14a}$$

$$q_b(t)=\varepsilon q_{b21}(T_0,T_1,T_2)+\varepsilon^2 q_{b22}(T_0,T_1,T_2)+\varepsilon^3 q_{b23}(T_0,T_1,T_2) \tag{14b}$$

$$q_c(t)=\varepsilon q_{c31}(T_0,T_1,T_2)+\varepsilon^2 q_{c32}(T_0,T_1,T_2)+\varepsilon^3 q_{c33}(T_0,T_1,T_2) \tag{14c}$$

Substituting Eq 14 into Eq 12, and equating the coefficients of ε^1, ε^2 and ε^3 in both sides of the equation, we obtain

Order ε^1

$$D_0^2 q_{a11} + \omega_a^2 q_{a11} = 0 \tag{15a}$$

$$D_0^2 q_{b11} + \omega_b^2 q_{b21} = 0 \tag{15b}$$

$$D_0^2 q_{c31} + \omega_c^2 q_{c31} = 0 \tag{15c}$$

Order ε^2

$$D_0^2 q_{a12} + \omega_a^2 q_{a12} = -2D_0 D_1 q_{a11} + e_4 q_{c31} + e_5 q_{b21}^2 + e_6 q_{a11}^2 \tag{16a}$$

$$D_0^2 q_{b22} + \omega_b^2 q_{b22} = -2D_0 D_1 q_{b21} + f_3 q_{a11} q_{b21} + f_4 q_{b21} q_{c31} \tag{16b}$$

$$D_0^2 q_{c32} + \omega_c^2 q_{c32} = -2D_0 D_1 q_{c31} + m_4 q_{a11} + m_5 q_{b21}^2 \tag{16c}$$

Order ε^3

$$\begin{aligned} D_0^2 q_{a13} + \omega_a^2 q_{a13} = &-2D_0 D_1 q_{a12} - \left(D_1^2 + 2D_0 D_2\right) q_{a11} - e_1 D_0 q_{a11} + e_3 H_b + e_4 q_{c32} \\ &+ 2e_5 q_{b21} q_{b22} + 2e_6 q_{a11} q_{a12} + e_7 q_{a11}^3 \end{aligned} \tag{17a}$$

$$\begin{aligned} D_0^2 q_{b23} + \omega_b^2 q_{b23} = &-2D_0 D_1 q_{b22} - \left(D_1^2 + 2D_0 D_2\right) q_{b21} - f_1 D_0 q_{b21} + f_3 q_{a11} q_{b22} \\ &+ f_3 q_{a12} q_{b21} + f_4 q_{b21} q_{c32} + f_4 q_{b22} q_{c31} + f_5 q_{21}^3 \end{aligned} \tag{17b}$$

$$\begin{aligned} D_0^2 q_{c33} + \omega_c^2 q_{c33} = &-2D_0 D_1 q_{c32} - \left(D_1^2 + 2D_0 D_2\right) q_{c31} - m_1 D_0 q_{c31} + m_3 H_b \\ &+ m_4 q_{a12} + 2m_5 q_{b21} q_{b22} \end{aligned} \tag{17c}$$

where $D_i = \partial / \partial T_i$

The complex solution of Eq 15 can be written as

$$q_{a11} = A_1\left(T_1, T_2\right) e^{i\omega_a T_0} + cc \tag{18a}$$

$$q_{b21} = A_2\left(T_1, T_2\right) e^{i\omega_b T_0} + cc \tag{18b}$$

$$q_{c31} = A_3\left(T_1, T_2\right) e^{i\omega_c T_0} + cc \tag{18c}$$

where $A_1(T_1,T_2)$, $A_2(T_1,T_2)$, $A_3(T_1,T_2)$ are unknown complex functions, and cc is the complex conjugate part to the preceding terms.

Substituting Eq 18 into Eq 16 yields

$$\begin{aligned} D_0^2 q_{a12} + \omega_a^2 q_{a12} = &-2\frac{\partial A_1}{\partial T_1} i\omega_a e^{i\omega_a T_0} + e_4 A_3 e^{i\omega_c T_0} + e_5 A_2^2 e^{2i\omega_b T_0} + A_2 \bar{A}_2 \\ &+ e_6 A_1^2 e^{2i\omega_a T_0} + cc \end{aligned} \tag{19a}$$

$$D_0^2 q_{b22} + \omega_b^2 q_{b22} = -2\frac{\partial A_2}{\partial T_1} i\omega_b e^{i\omega_b T_0} + f_3 A_1 A_2 e^{i(\omega_a+\omega_b)T_0} + f_3 A_1 \bar{A}_2 e^{i(\omega_a-\omega_b)T_0} + f_4 A_2 A_3 e^{i(\omega_b+\omega_c)T_0} + f_4 \bar{A}_2 A_3 e^{i(\omega_c-\omega_b)T_0} + cc \tag{19b}$$

$$D_0^2 q_{c32} + \omega_c^2 q_{c32} = -2\frac{\partial A_3}{\partial T_1} i\omega_c e^{i\omega_c T_0} + m_4 A_1 e^{i\omega_a T_0} + m_5 A_2^2 e^{2i\omega_b T_0} + A_2 \bar{A}_2 + cc \tag{19c}$$

When the resonance does not occur, for the elimination of secular terms, we obtain

$$\frac{\partial A_i}{\partial T_1} = 0, \quad i = 1、2、3 \tag{20}$$

Solving Eq 19, we can get

$$q_{a12} = \frac{e_4 A_3}{\omega_a^2 - \omega_c^2} e^{i\omega_c T_0} + \frac{e_5 A_2^2}{\omega_a^2 - 4\omega_b^2} e^{2i\omega_b T_0} + \frac{A_2 \bar{A}_2}{\omega_a^2} - \frac{e_6 A_1^2}{3\omega_a^2} e^{2i\omega_a T_0} + cc \tag{21a}$$

$$q_{b22} = \frac{f_3 A_1 A_2}{\omega_b^2 - (\omega_a + \omega_b)^2} e^{i(\omega_a+\omega_b)T_0} + \frac{f_3 A_1 \bar{A}_2}{\omega_b^2 - (\omega_a - \omega_b)^2} e^{i(\omega_a-\omega_b)T_0} + \frac{f_4 A_2 A_3}{\omega_b^2 - (\omega_b + \omega_c)^2} e^{i(\omega_b+\omega_c)T_0} + \frac{f_4 \bar{A}_2 A_3}{\omega_b^2 - (\omega_c - \omega_b)^2} e^{i(\omega_c-\omega_b)T_0} + cc \tag{21b}$$

$$q_{c32} = \frac{m_4 A_1}{\omega_c^2 - \omega_a^2} e^{i\omega_a T_0} + \frac{m_5 A_2^2}{\omega_c^2 - 4\omega_b^2} e^{2i\omega_b T_0} + \frac{A_2 \bar{A}_2}{\omega_a^2} + cc \tag{21c}$$

Substituting Eqs 18 and 21 into Eq 17 yields

$$D_0^2 q_{a13} + \omega_a^2 q_{a13} = h_1 e^{i\omega_a T_0} + h_2 e^{3i\omega_a T_0} + h_3 e^{i\omega_c T_0} + h_4 e^{2i\omega_b T_0} + h_5 e^{i(\omega_a+2\omega_b)T_0} + h_6 e^{i(2\omega_b-\omega_a)T_0} + h_7 e^{i(2\omega_b+\omega_c)T_0} + h_8 e^{i(\omega_c-2\omega_b)T_0} + h_9 e^{i(\omega_a+\omega_c)T_0} + h_{10} e^{i(\omega_a-\omega_c)T_0} + h_{11} + cc \tag{22a}$$

$$D_0^2 q_{b23} + \omega_b^2 q_{b23} = j_1 e^{i\omega_b T_0} + j_2 e^{3i\omega_b T_0} + j_3 e^{i(\omega_b+\omega_c)T_0} + j_4 e^{i(\omega_b+\omega_a)T_0} + j_5 e^{i(\omega_b-\omega_a)T_0} + j_6 e^{i(\omega_b-\omega_c)T_0} + j_7 e^{i(2\omega_a+\omega_b)T_0} + j_8 e^{i(\omega_b+2\omega_c)T_0} + j_9 e^{i(2\omega_c-\omega_b)T_0} + j_{10} e^{i(2\omega_a-\omega_b)T_0} + j_{11} e^{i(\omega_a+\omega_b+\omega_c)T_0} + j_{12} e^{i(\omega_b+\omega_c-\omega_a)T_0} + j_{13} e^{i(\omega_a+\omega_c-\omega_b)T_0} + j_{14} e^{i(\omega_a+\omega_b-\omega_c)T_0} + cc \tag{22b}$$

$$D_0^2 q_{c33} + \omega_c^2 q_{b33} = k_1 e^{i\omega_c T_0} + k_2 e^{2i\omega_b T_0} + k_3 e^{i\omega_a T_0} + k_4 e^{2i\omega_a T_0} + k_5 e^{i(\omega_a+2\omega_b)T_0} + k_6 e^{i(2\omega_b+\omega_c)T_0} + k_7 e^{i(2\omega_b-\omega_a)T_0} + k_8 e^{i(2\omega_b-\omega_c)T_0} + k_9 + cc \tag{22c}$$

The coefficients presented in Eq 22 are interpreted in the Appendix B.

From Eq 22, we can know that there are many kinds of internal resonance when the frequencies of the main cable, sling and beam satisfy some special relationship, such as 1:1 ($\omega_a \approx$

ω_c) and 1:2 ($\omega_a \approx 2\omega_b$, $\omega_c \approx 2\omega_b$) internal resonance. This paper only deals with the situation when the sum of ω_a and ω_c approaches two times of ω_b ($\omega_a + \omega_c \approx 2\omega_b$).

Introducing a detuning parameter σ and supposing

$$\omega_c + \omega_a = 2\omega_b + \varepsilon^2\sigma \tag{23}$$

Substituting Eq 23 into Eq 22 and eliminating the secular terms yields

$$\begin{aligned}&-2\frac{\partial A_1}{\partial T_2} iw_a - \mu_a A_1 iw_a + \frac{e_4 m_4 A_1}{w_c^2 - w_a^2} + \frac{2e_5 f_3 A_1 A_2 \bar{A}_2}{w_b^2 - (w_a + w_b)^2} + \frac{2e_5 f_3 A_1 A_2 \bar{A}_2}{w_b^2 - (w_a - w_b)^2} \\ &+ \frac{4e_6 e_5 A_1 A_2 \bar{A}_2}{w_a^2} - \frac{2e_6^2 A_1^2 \bar{A}_1}{3w_a^2} + \frac{4e_6^2 A_1^2 \bar{A}_1}{w_a^2} + 3e_7 A_1^2 \bar{A}_1 + \frac{2e_5 f_4 A_2^2 \bar{A}_3}{w_b^2 - (w_c - w_b)^2} e^{-i\sigma T_2} = 0\end{aligned} \tag{24a}$$

$$\begin{aligned}&-2\frac{\partial A_2}{\partial T_2} i\omega_b - \mu_b A_2 iw_b + \frac{f_3^2 A_1 \bar{A}_1 A_2}{w_b^2 - (w_a + w_b)^2} + \frac{f_3^2 A_1 \bar{A}_1 A_2}{w_b^2 - (w_a - w_b)^2} + \frac{f_3 e_5 A_2^2 \bar{A}_2}{w_a^2 - 4w_b^2} \\ &+ \frac{2 f_3 e_5 A_2^2 \bar{A}_2}{w_a^2} + \frac{2 f_3 e_6 A_1 \bar{A}_1 A_2}{w_a^2} + \frac{f_4 m_5 \bar{A}_2 A_2^2}{w_c^2 - 4w_b^2} + \frac{2 f_4 m_5 A_2^2 \bar{A}_2}{w_a^2} + \frac{f_4^2 A_2 A_3 \bar{A}_3}{w_b^2 - (w_b + w_c)^2} \\ &+ \frac{f_4^2 A_2 \bar{A}_3 A_3}{w_b^2 - (w_c - w_b)^2} + 3 f_5 A_2^2 \bar{A}_2 + \left[\frac{f_3 f_4 A_1 \bar{A}_2 A_3}{w_b^2 - (w_c - w_b)^2} + \frac{f_3 f_4 A_1 \bar{A}_2 A_3}{w_b^2 - (w_a - w_b)^2} \right] e^{i\sigma T_2} = 0\end{aligned} \tag{24b}$$

$$\begin{aligned}&-2\frac{\partial A_3}{\partial T_2} iw_c - \mu_c A_3 iw_c + \frac{m_4 e_4 A_3}{w_a^2 - w_c^2} + \frac{2m_5 f_4 \bar{A}_2 A_2 A_3}{w_b^2 - (w_b + w_c)^2} + \frac{2m_5 f_4 A_2 \bar{A}_2 A_3}{w_b^2 - (w_c - w_b)^2} \\ &+ \frac{2m_5 f_3 \bar{A}_1 A_2^2}{w_b^2 - (w_a - w_b)^2} e^{-i\sigma T_2} = 0\end{aligned} \tag{24c}$$

The complex functions can be expressed as

$$A_i(T_2) = a_i(T_2) e^{i\theta_i(T_2)}, \quad i = 1,2,3 \tag{25}$$

where a_i, θ_i are real functions with respect to T_2.

Substituting Eq 25 into Eq 24, and setting the real and imaginary parts to be zero, respectively, we then get

$$2w_a a_1' + \mu_a w_a a_1 + \frac{2e_5 f_4 a_2^2 a_3}{w_b^2 - (w_c - w_b)^2} \sin\lambda = 0 \tag{26a}$$

$$2w_b a_2' + \mu_b w_b a_2 - \left[\frac{f_3 f_4 a_1 a_2 a_3}{w_b^2 - (w_c - w_b)^2} + \frac{f_3 f_4 a_1 a_2 a_3}{w_b^2 - (w_a - w_b)^2} \right] \sin\lambda = 0 \tag{26b}$$

$$2w_c a_3' + \mu_c w_c a_3 + \frac{2m_5 f_3 a_1 a_2^2}{w_b^2 - (w_a - w_b)^2} \sin\lambda = 0 \tag{26c}$$

$$2w_a a_1\theta_1' + \frac{e_4 m_4 a_1}{w_c^2 - w_a^2} + \frac{2e_5 f_3 a_1 a_2^2}{w_b^2 - (w_a + w_b)^2} + \frac{2e_5 f_3 a_1 a_2^2}{w_b^2 - (w_a - w_b)^2} + \frac{4e_6 e_5 a_1 a_2^2}{w_a^2}$$
$$- \frac{2e_6^2 a_1^3}{3w_a^2} + \frac{4e_6^2 a_1^3}{w_a^2} + 3e_7 a_1^3 + \frac{2e_5 f_4 a_2^2 a_3}{w_b^2 - (w_c - w_b)^2}\cos\lambda = 0 \tag{26d}$$

$$2w_b a_2\theta_2' + \frac{f_3^2 a_1^2 a_2}{w_b^2 - (w_a + w_b)^2} + \frac{f_3^2 a_1^2 a_2}{w_b^2 - (w_a - w_b)^2} + \frac{f_3 e_5 a_2^3}{w_a^2 - 4w_b^2}$$
$$+ \frac{2f_3 e_5 a_2^3}{w_a^2} + \frac{2f_3 e_6 a_1^2 a_2}{w_a^2} + \frac{f_4 m_5 a_2^3}{w_c^2 - 4w_b^2} + \frac{2f_4 m_5 a_2^3}{w_a^2} + \frac{f_4^2 a_2 a_3^2}{w_b^2 - (w_b + w_c)^2}$$
$$+ \frac{f_4^2 a_2 a_3^2}{w_b^2 - (w_c - w_b)^2} + 3f_5 a_2^3 + \left[\frac{f_3 f_4 a_1 a_2 a_3}{w_b^2 - (w_c - w_b)^2} + \frac{f_3 f_4 a_1 a_2 a_3}{w_b^2 - (w_a - w_b)^2}\right]\cos\lambda = 0 \tag{26e}$$

$$2w_c a_3\theta_3' + \frac{m_4 e_4 a_3}{w_a^2 - w_c^2} + \frac{2m_5 f_4 a_2^2 a_3}{w_b^2 - (w_b + w_c)^2} + \frac{2m_5 f_4 a_2^2 a_3}{w_b^2 - (w_c - w_b)^2}$$
$$+ \frac{2m_5 f_3 a_1 a_2^2}{w_b^2 - (w_a - w_b)^2}\cos\lambda = 0 \tag{26f}$$

where

$$\lambda = \theta_1 + \theta_3 - 2\theta_2 + \delta T_2 \tag{27}$$

From Eq 26, if not considering the damping of the system, then we can obtain

$$\frac{f_3}{2e_5}a_1^2 + \frac{w_b}{w_a}a_2^2 + \frac{f_4 w_c}{2m_5 w_a}a_3^2 = E \tag{28}$$

where E is a constant of integration proportional to the initial energy of the system. If f_3/e_5 and f_4/m_5 have the same sign and E is positive definite, Eq 28 shows that a_1, a_2 and a_3 are always bounded. In the paper, we assume that the system does not contain regenerative elements [34], so that f_3/e_5 and f_4/m_5 have the same sign.

When considering the damping coefficients of the coupled structure, a_1, a_2 and a_3 are also bounded, but E will decrease with time, which will show in the following section.

4. Numerical results and discussion

In the following numerical investigations, the basis functions used here are [35–37]

$$\phi(x_i) = \sin(\pi x_i), \quad i = a, b, c \tag{29}$$

which satisfy the boundary conditions in Eq 9.

4.1. Frequency of the sling

In the section, ten slings of Aizhai suspension bridge are taking as an example, the fundamental parameters of which are listed in Table 1. And then, a full bridge model with MIDAS CIVIL and a single sling model with ABAQUS are made to obtain the finite element values of the frequencies of the slings. Furthermore, we have measured the slings at the bridge construction site to get the measured values of the frequencies of the slings. At last, the frequencies of the slings obtained by Eq A9 are compared with those are measured and got by finite element models.

The calculation process of the finite element value of the frequency of the sling is: at first, a full bridge model is built with MIDAS CIVIL and from the model, we can get the cable force of the sling at the service stage of the bridge; then the cable force of one sling is used in the single cable model, which is built with ABAQUS, and from the model, we can get the frequency of the sling. In the full bridge model, the suspension and the sling are simulated with tension-only truss element, the beam and the tower are built with beam element. In the single cable model, the sling is simulated with the type of T3D2 of truss element. The screenshot of the finite element model of Aizhai suspension bridge is shown as follows, and the ten slings have been marked in red, the NO. is J01 to J10 from left to right.

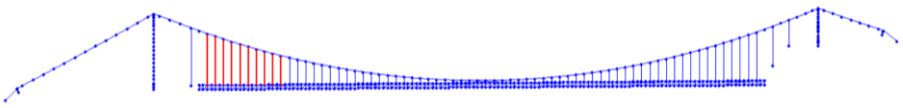

Figure 2. The finite element model of Aizhai suspension bridge.

Table 1. Parameters of ten slings of Aizhai suspension bridge.

Parameters	J01	J02	J03	J04	J05	J06	J07	J08	J09	J10
Length (m)	90.59	85.55	80.66	75.92	71.34	66.91	62.64	58.51	54.54	50.73
Mass (kg/m)	34.5	34.5	16.9	16.9	16.9	16.9	16.9	16.9	16.9	16.9
Cable force (N)	2.27e6	2.07e6	2.06e6	2.05e6	2.05e6	2.04e6	2.04e6	2.03e6	2.03e6	2.02e6

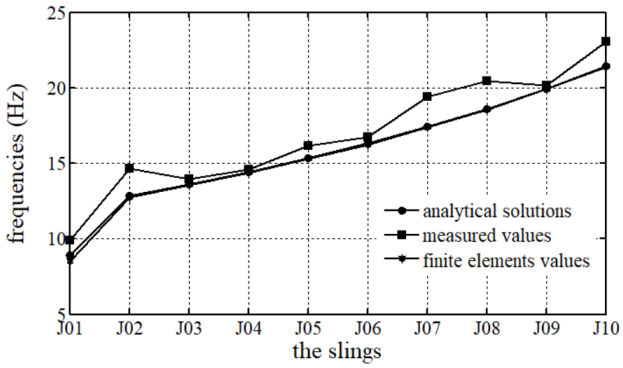

Figure 3. Comparison of the analytical solutions with measured values and finite element values of frequencies of the ten slings.

Figure 3 shows the validity of the reduced models in Eq 10 for deriving formulas of this paper. A good agreement can be obtained. The frequency differences of analytical solutions with measured values and finite element values are in an allowance range of 5%.

4.2. Time history of amplitude

The initial parameters of the coupled structure are shown in Table 2.

Table 2. The initial parameters of the coupled structure.

M_a	1214.9 kg/m	M_b	34.5 kg/m	M_c	3256.5 kg/m
l_a	327.1 m	l_b	90.59 m	l_c	327.1 m
E_a	1.96×10^{11} Pa	E_b	$1.15e \times 10^{11}$ Pa	E_c	2.1×10^{11} Pa
H_a	1.37×10^{8} N	H_b	2.28×10^{6} N	I_c	98.9 m^4
A_a	0.464621 m^2	A_b	0.003977 m^2		
l_p	39.25 m	l_q	39.25 m		

Time history of amplitude of the summation resonance of the coupled structure is analyzed. According to the parameters given above, the frequencies of the main cable, sling and beam will be ω_a = 4.456, ω_b = 8.911, ω_c = 13.367 (Example A), which satisfies the condition of summation resonance of Eq 23 and $\xi^2\sigma$ = 0. Then, via Eq 26, time history of amplitude can be obtained and shown in Figures 4–5. Figure 4 does not consider the damping coefficients of the coupled structure, while Figure 5 considers four kinds of damping coefficient of the sling. Furthermore, a_1^0, a_2^0, a_3^0 and t^0 in Figure 4 stand for the first peaks of the amplitudes of the main cable, sling, beam; t^0 stands for the time when a_1, a_2, a_3 reach the first peaks, which we call it triggering time in the following sections.

From Figure 4 the following can be observed: Without damping, the summation resonance of the coupled structure is periodical, stable and bounded; total energy of the coupled structure is conserved and transferring among the main cable, sling and beam, which has typical characteristic of "beat"; the main cable and beam are energy provider while the sling is energy recipient in the first half cycle of each cycle.

Figure 5 shows with damping, the summation resonance of the coupled structure still has the characteristic of "beat", but total energy of the coupled structure is gradually consumed with time going on. For any kind of damping, though we only take the damping coefficient of the sling into account, the peaks of the amplitudes of the main cable and beam also change. Therefore, we can conclude that due to the internal resonance, we can adjust the attenuation law of one degree by changing the damping coefficient of another degree. As the damping coefficient of the sling increases, the first peaks of the amplitudes of the main cable, sling, beam decrease and the triggering time becomes larger. It shows the inhibitory effect of the damping on the coupled structure increases. Thus, we can get that the increasing damping not only gradually decreases the amplitude of the coupled structure, but also makes the energy exchange become slower.

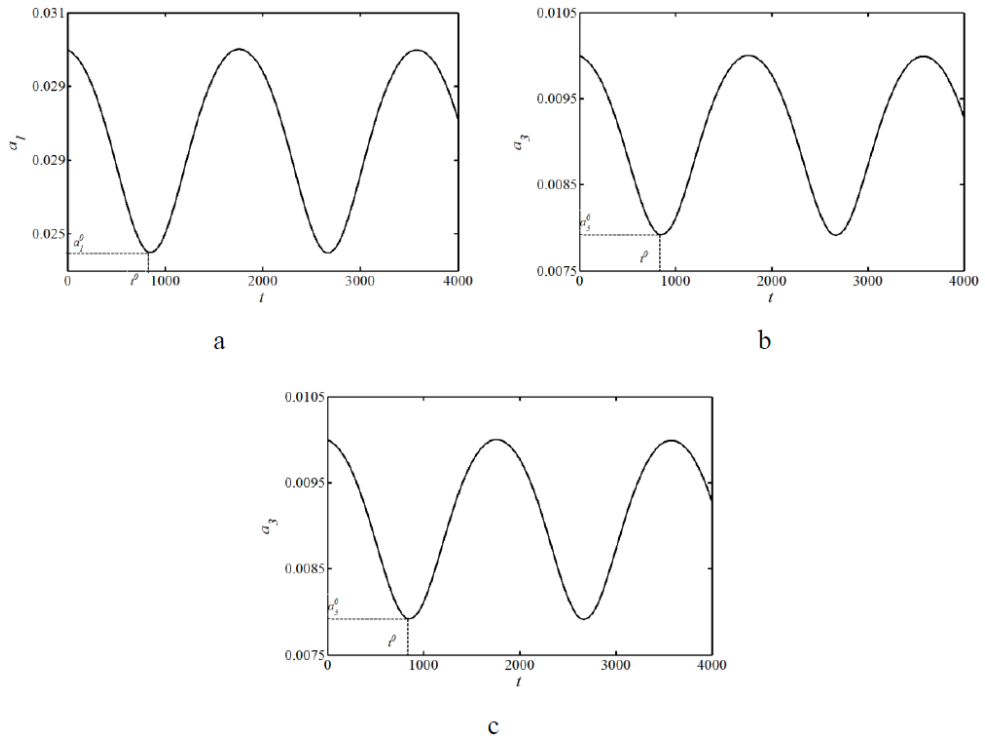

Figure 4. Time history of amplitude of summation resonance of the coupled structure without damping: a: main cable; b: sling; c: beam.

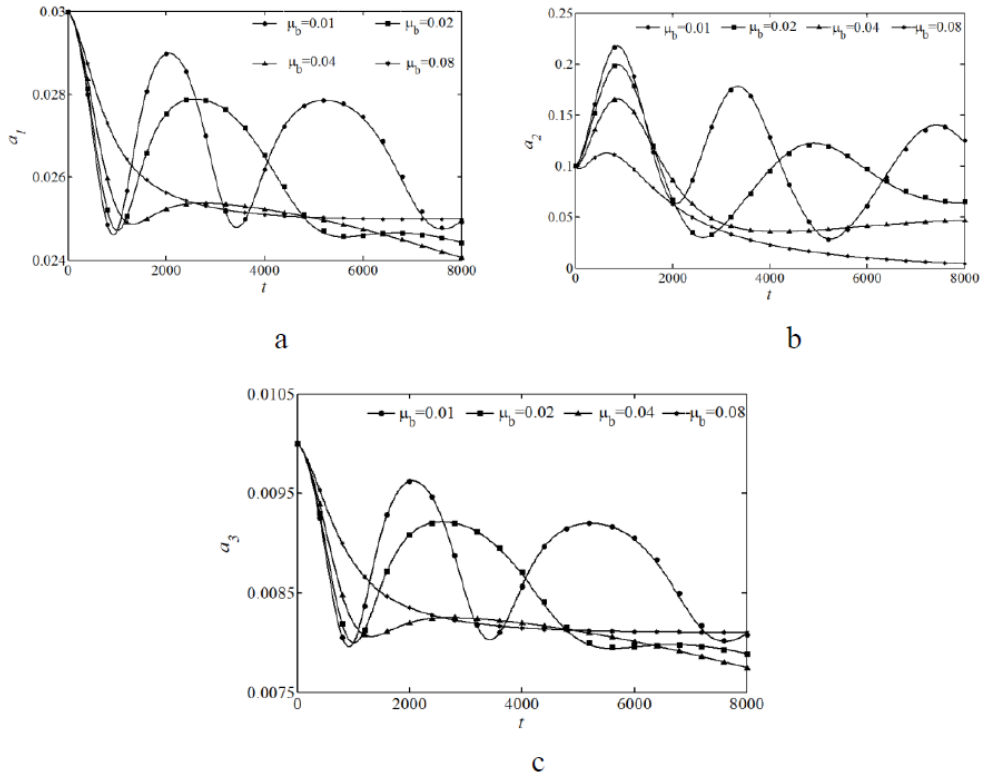

Figure 5. Time history of amplitude of summation resonance of the coupled structure with damping (μ_b = 0.01, 0.02, 0.04, 0.08): a: main cable; b: sling; c: beam.

4.3. Time history of displacement

In the section, numerical investigations are used directly for the dynamic equilibrium equations to complement and verify the analytical solutions above. The initial solutions are set to $Dq_a = 0$, $Dq_b = 0$, $Dq_c = 0$, $q_a = 0.001$, $q_b = 0.1$, $q_c = 0.1$, where D indicates differentiation with respect to time t. By fourth-order Runge-Kutta method, time history of displacement of summation resonance with damping and without damping can be obtained and as shown in Figures 6–7.

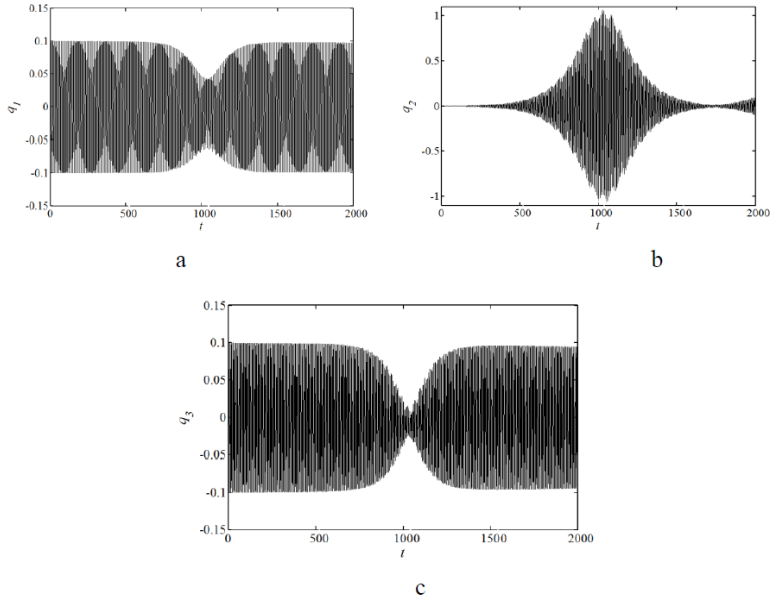

Figure 6. Time history of displacement of summation resonance of the coupled structure without damping: a: main cable; b: sling; c: beam.

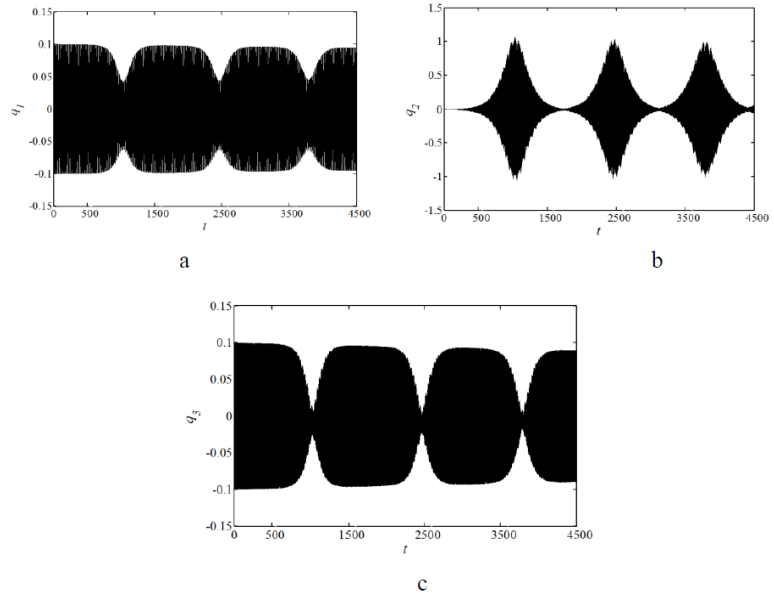

Figure 7. Time history of displacement of summation resonance of the coupled structure with damping: a: main cable; b: sling; c: beam.

From Figures 6–7, it can be observed that with and without damping, the displacement curves of the main cable, sling and beam have the characteristics of "beat"; the main cable and beam are energy provider and the sling is energy recipient in the first half cycle of each cycle of amplitude; total energy of the coupled structure is transferring among the main cable, sling and beam; total energy of the coupled structure is conserved, while with damping, total energy decreases with time.

The conclusions obtained above well verify the results got in Section 4.2, and further demonstrate the correctness of theoretical analysis obtained by multiple scales method.

4.4. Amplitude-frequency response

4.1.1. $(a_1^0, a_2^0, a_3^0, t^0) - \sigma$

Given that some parameters of the coupled structure always vary, the sum of the frequencies of the main cable and beam is not always just two times of that of the sling. Therefore, based on the previous section, we slightly change the initial parameters of the coupled structure to make $\omega_a + \omega_c$ slightly deviate from $2\omega_b$. Then, the first peaks of the amplitudes of the coupled structure as functions of frequency ($a_1^0, a_2^0, a_3^0 - \sigma$) and triggering time as function of frequency ($t^0 - \sigma$) can be obtained and shown in Figure 8.

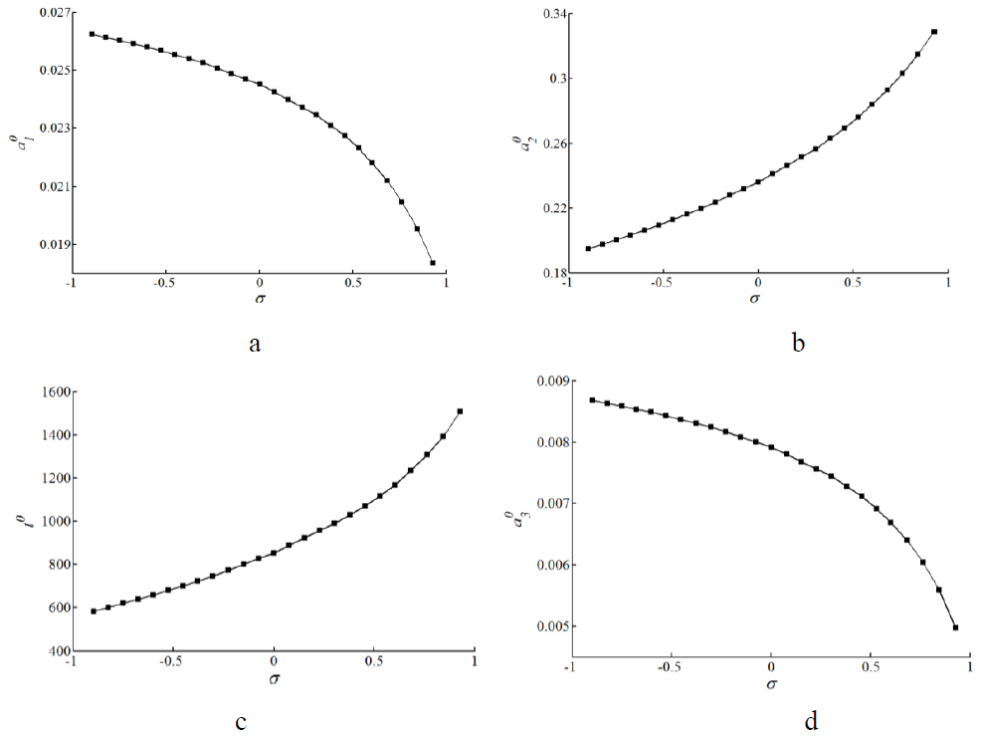

Figure 8. The first peaks of the amplitudes and triggering time as functions of frequency: a: main cable; b: sling; c: beam; d: triggering time

From Figure 8, it can be observed that all the curves are single-valued and nonlinear. With the increase of σ, the first peaks of amplitudes of the main cable and beam decrease, while the first

peak of the sling and triggering time increases. It means as σ increases, the main cable and beam provide more energy and the sling receive more energy, but the energy exchange becomes slower.

4.1.2. $(a_1^0, a_2^0, a_3^0, t^0) - (\omega_c - \omega_a)$

Changing the initial parameters of the coupled structure to make the frequencies of the main cable and beam to $\omega_a = 8.911$, $\omega_c = 8.911$ (Example B) and comparing the numerical results with that of Section 4.2 (without damping).

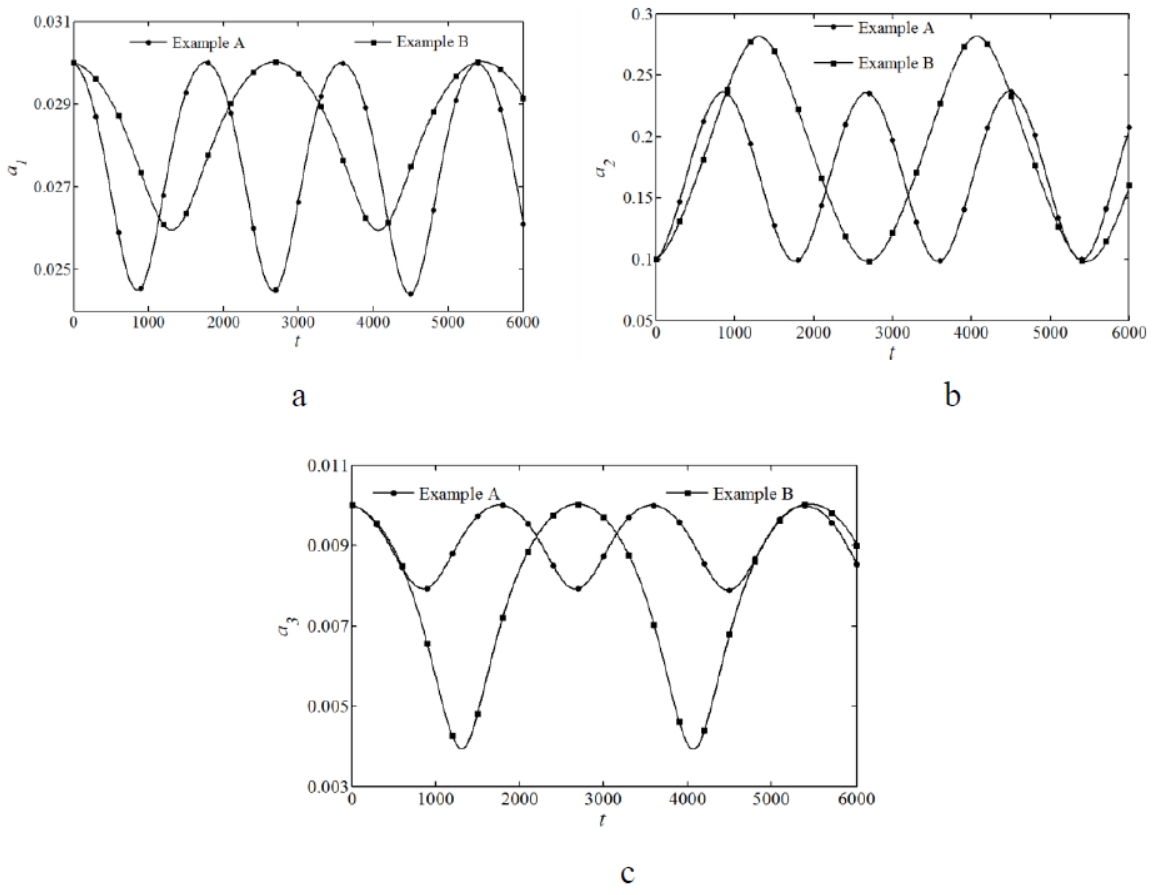

Figure 9. Comparison of time history of amplitude of Example A and Example B (without damping): a: main cable; b: sling; c: beam.

Figure 9 shows under the condition of summation resonance, different frequency combinations of the main cable (ω_a) and beam (ω_c) get different peaks (a_1^0, a_2^0, a_3^0) and triggering time (t^0). The following section will discuss the effect of the frequency combination of the main cable and beam on a_1^0, a_2^0, a_3^0 and t^0.

Many kinds of frequency combinations of the coupled structure are analyzed. Due to space limitations, only some of them are shown in Table 3. The influence curves of the frequency combination on a_1^0, a_2^0, a_3^0 and t^0 are obtained and shown in Figure 10 (without damping).

Table 3. The frequency combinations of the coupled structure.

ω_a	ω_b	ω_c	$\omega_c - \omega_a$
8.911	8.911	8.911	0
7.911	8.911	9.911	2
6.911	8.911	10.911	4
5.911	8.911	11.911	6
4.911	8.911	12.911	8
3.911	8.911	13.911	10
2.911	8.911	14.911	12
1.911	8.911	15.911	14

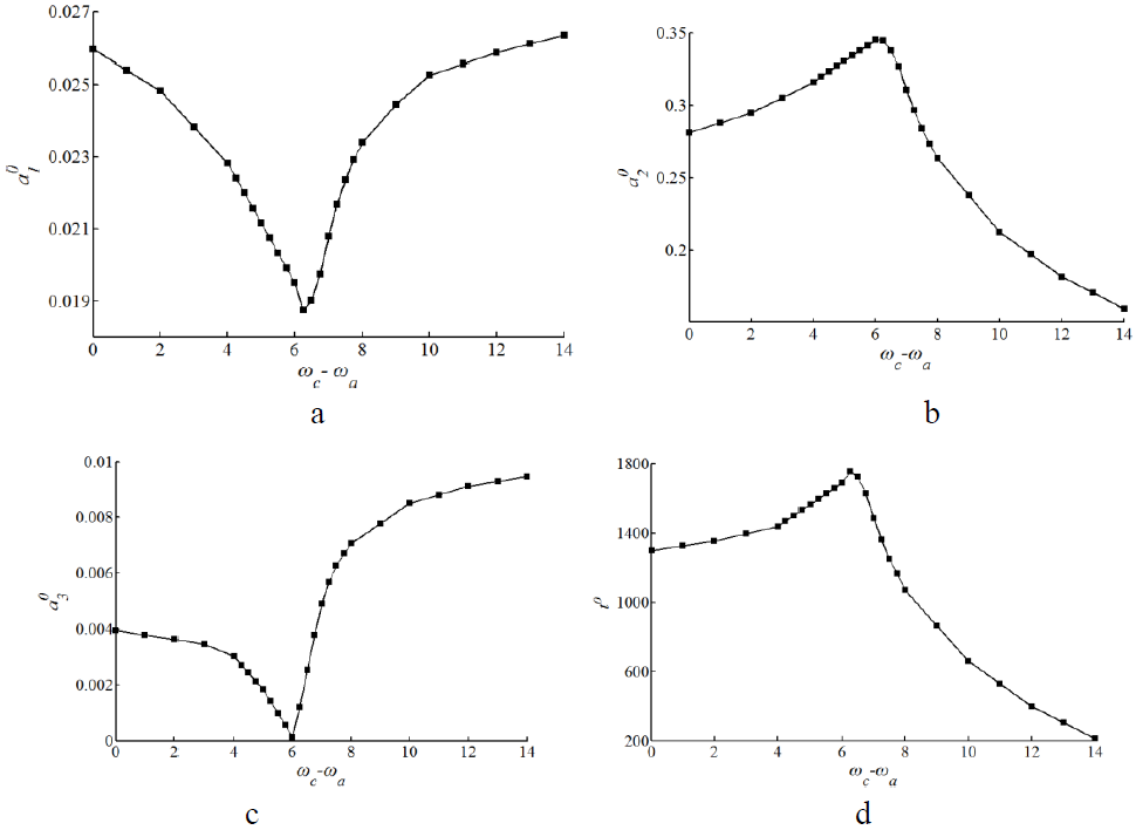

Figure 10 The effect of the frequency combination of the main cable and beam on peaks and triggering time of the amplitude-time responses: a: main cable; b: sling; c: beam; d: triggering time.

Figure 10 shows with the increase of $\omega_c - \omega_a$, $a_1{}^0$ and $a_3{}^0$ decrease first and then increase, while $a_2{}^0$ and t^0 increase first and then decrease, there exists inflection point when $\omega_c - \omega_a$ gets the value of about 6.2. Thus, it indicates as $\omega_c - \omega_a$ increases, the main cable and beam provide more energy with the sling until the inflection point and after then less energy will be provided. In the inflection point, the sling receives the most energy, having the biggest amplitude and the coupled structure has the longest triggering time, showing the energy exchange is the slowest.

5. Conclusions

The paper investigates free vibration of summation resonance of the suspended–cable–stayed beam. At first, a 3-DOF model is built, which treated the main cable and the sling as nonlinear taut string and the beam as Euler beam; then, Hamilton's principle and multiple scales method are used to derive and solve the dynamic equilibrium equations; at last, numerical integration method is used to discuss the nonlinear characteristics of the coupled structure. We can yield the following conclusions:

1. Without damping, the free vibration of summation resonance of the coupled structure will be periodical, stable and bounded; total energy of the coupled structure is conserved and transferring among the main cable, sling and beam, which has typical characteristic of "beat"; the main cable and beam are energy provider and the sling is energy recipient in the first half cycle of each cycle.
2. With damping, total energy of the coupled structure is gradually consumed; due to the internal resonance, we can adjust the attenuation law of one degree by changing the damping coefficient of another degree; as the damping of the coupled structure increases, the peaks of the amplitudes decrease and the energy exchange becomes slower.
3. As σ increases, the main cable and beam provide more energy and the sling receive more energy, but the energy exchange becomes slower.
4. As the difference of the frequency of the beam and main cable ($\omega_c - \omega_a$) increases, the main cable and beam provide more energy with the sling until the inflection point and after then less energy will be provided. In the inflection point, the sling receives the most energy and the energy exchange is the slowest.

Acknowledgments

All the authors gratefully acknowledge the support of the National Natural Science of Foundation of China (No.51678247), Natural Science Foundation of Hebei Province (E2019210311) and the 'Cooperative Innovation Center of Disaster Prevention and Mitigation for Large Infrastructure in Hebei province (Shijiazhuang Tiedao University)'.

Conflict of interest

The authors declare that they have no conflict of interest in this paper.

References

1. K. Takahashi and Y. Konishi, Non-linear vibrations of cables in three dimensions, Part II: out-of-plane vibrations under in-plane sinusoidally time-varying load, *J. Sound Vib.*, **118** (1987), 85–97.
2. J. L. Lilien and A. P. Da Costa, Vibration amplitudes caused by parametric excitation of cable stayed structures, *J. Sound Vib.*, **174** (1994), 69–90.

3. H. N. Arafat and A. H. Nayfeh, Non-linear responses of suspended cables to primary resonance excitations, *J. Sound Vib.*, **266** (2003), 325–354.
4. H. Wang, T. Y. Tao, R. Zhou, et al., Parameter sensitivity study on flutter stability of a long-span triple-tower suspension bridge, *J. Wind Eng. Ind. Aerod.*, **128** (2014), 12–21.
5. T. Grigorjeva and Z. Kamaitis, Numerical analysis of the effects of the bending stiffness of the cable and the mass of structural members on free vibrations of suspension bridges, *J. Civ. Eng. Manag.*, **21** (2015), 948–957.
6. C. G. Koh and Y. Rong, Dynamic analysis of large displacement cable motion with experimental verification, *J. Sound Vib.*, **272** (2004), 183–206.
7. M. H. EI Ouni and N. B. Kahla, Nonlinear dynamic analysis of a cable under first and second order parametric excitations, *J. Civ. Eng. Manag.*, **18** (2012), 557–567.
8. D. Xue, Y. Liu, J. He, et al., Experimental study and numerical analysis of a composite truss joint, *J. Constr Steel Res.*, **67** (2011), 957–964.
9. K. Takahashi, Dynamic stability of cables subjected to an axial periodic load, *J. Sound Vib*., **144** (1991), 323–330.
10. A. P. Da Costa and J. A. C. Martins, Oscillations of bridge stay cables induced by periodic motions of deck and/or towers, *J. Eng. Mech.*, **122** (1996), 613–622.
11. H. Chen, D. Zuo, Z. Zhang, et al., Bifurcations and chaotic dynamics in suspended cables under simultaneous parametric and external excitations, *Nonlinear Dyn.*, **62** (2010), 623–646.
12. D. Zulli and A. Luongo, Nonlinear energy sink to control vibrations of an internally nonresonant elastic string, *Meccanica*, **50** (2014), 781–794.
13. B. N. Sun and Z. G. Wang, Cable oscillation induced by parametric excitation in cable-stayed bridges, *J. Zhejiang Univ-sc A*, **4** (2003), 13–20.
14. Y. Fujino and P. Warnitchai, An experimental and analytical study of auto parametric resonance in a 3-DOF model of cable-stayed-beam, *Nonlinear Dyn.*, **4** (1993), 111–138.
15. Y. Xia and Y. Fujino, Auto-parametric vibration of a cable-stayed-beam structure under random excitation, *J. Eng. Mech.*, **132** (2006), 279–286.
16. Y. Xia, Q. X. Wu, Y. L. Xu, et al., Verification of a cable element for cable parametric vibration of one-cable-beam system subject to harmonic excitation and random excitation, *Adv. Struct. Eng.*, **14** (2011), 589–595.
17. V. Gattulli and M. Lepidi, Nonlinear interactions in the planar dynamics of cable-stayed beam, *Int J. Solids Struct.*, **40** (2003), 4729–4748.
18. V. Gattulli and M. Morandini, A parametric analytical model for non-linear dynamics in cable-stayed beam, *Earthq. Eng. Struct. D.*, **31** (2002), 1281–1300.
19. V. Gattulli and M. Lepidi, One-to-two global-local interaction in a cable-stayed beam observed through analytical, finite element and experimental models, *Int. J. Nonlin Mech.*, **40** (2005), 571–588.
20. Z. Wang, C. Sun, Y. Zhao, et. al., Modeling and nonlinear modal characteristics of the cable-stayed beam, *Eur. J. Mech- A-Solid*, **47** (2014), 58–69.
21. M. H. Wei, K. Lin, L. Jin, et. al., Nonlinear dynamics of a cable-stayed beam driven by sub-harmonic and principal parametric resonance, *Int. J. Mech. Sci.*, **110** (2016), 78–93.

22. Z. W. Wang and T. J. Li, Nonlinear dynamic analysis of parametrically excited space cable-beam structures due to thermal loads, *Eng. Struct.*, **83** (2015), 50–61.
23. H. J. Kang, H. P. Zhu, Y. Y. Zhao, et al., In-plane non-linear dynamics of the stay cables, *Nonlinear Dyn.*, **73** (20136), 54–59.
24. Y. Y. Zhao and H. J. Kang, In-plane free vibration analysis of cable-arch structure, *J. Sound Vib.*, **312** (2008), 363–379.
25. H. J. Kang, Y. Y. Zhao and H. P. Zhu, Out-of-plane free vibration analysis of a cable-arch structure, *J. Sound Vib.*, **332** (2013), 907–921.
26. A. H. Nayfeh and D. T. Mook, Nonlinear Oscillations, John Wiley & Sons, (1979), 71–79.
27. J. R. Zhao, Y. G. Tang and L. Q. Liu, Study on the sum type combination resonance responses of a classic Spar platform, *Ocean Eng.*, **27** (2009), 23–30.
28. L. Q. Chen, J. W. Zu and J. Wu, Steady-state response of the parametrically excited axially moving string constituted by the Boltzmann superposition principle, *Acta Mech.*, **162** (2003), 143–155.
29. Q. X. Wu, L. Liu and B. C. Chen, Theoretical equations of in-plane natural vibration for cables considering bending stiffness, *Eng. Mech.*, **27** (2010), 9–27.
30. M. Irvine, Cable Structures, The MIT Series in Structural Mechanics, (1981).
31. Japan Society of Civil Engineers, Basic and application of cable and space structures, Maruzen, Japan: JSCE, (1999).
32. G. H. Li, H. F. Xiang and Z. Y. Shen, Stability and vibration of bridge structures, China Railway Publishing House, (2010), 132–134.
33. N. J. Gimsing and C. T. Georgakis, Cable supported bridges: concept and design. 3th ed, John Wiley & Sons, (2011), 220–225.
34. A. H. Nayfeh and D. T. Mook, Nonlinear Oscillation, John Wiley & Sons, (1979).
35. M. Al-Qassab and S. Nair, Wavelet-Galerkin method for the free vibrations of an elastic cable carrying an attached mass, *J. Sound Vib.*, **270** (2004), 191–206.
36. S. H. Zhou, G. Q. Song, Z. H. Ren, et al., Nonlinear analysis of a parametrically excited beam with intermediate support by using Multi-dimensional incremental harmonic balance method, *Chaos, Solitons & Fractals*, **93** (2016), 207–222.
37. P. J. Li, R. H. Wang and N. J. Ma, Analytic algorithm of transverse vibration frequency of cables with intermediate flexible supports, *J. South China Univ T.*, **40** (2012), 7–18.

AIMS Press